Brain Stimulation 12 (2019) 1127–1134

Contents lists available at ScienceDirect

Brain Stimulation

journal homepage: http://www.journals.elsevier.com/brain-stimulation

# Directional stimulation of subthalamic nucleus sweet spot predicts clinical efficacy: Proof of concept

T.A. Khoa Nguyen [a, 1], Andreas Nowacki [a, *, 1], Ines Debove [b], Katrin Petermann [b], Gerd Tinkhauser [b, c], Roland Wiest [d], Michael Schüpbach [b], Paul Krack [b], Claudio Pollo [a]

[a] Department of Neurosurgery, Inselspital, University Hospital Bern, University of Bern, Bern, Switzerland
[b] Department of Neurology, Inselspital, University Hospital Bern, University of Bern, Bern, Switzerland
[c] Medical Research Council Brain Network Dynamics Unit, Nuffield Department of Clinical Neurosciences, University of Oxford, United Kingdom
[d] Department of Diagnostic and Interventional Neuroradiology, Inselspital, University Hospital Bern, and University of Bern, Bern, Switzerland

ARTICLE INFO

*Article history:*
Received 16 November 2018
Received in revised form
30 March 2019
Accepted 2 May 2019
Available online 17 May 2019

*Keywords:*
Deep brain stimulation
Directional electrode
Parkinson's disease
Volume of tissue activated
Probabilistic stimulation map

ABSTRACT

*Background:* Directional deep brain stimulation (dDBS) of the subthalamic nucleus for Parkinson's disease (PD) increases the therapeutic window. However, empirical programming of the neurostimulator becomes more complex given the increasing number of stimulation parameters. A better understanding of dDBS is needed to improve therapy and help guide postoperative programming.
*Objective:* To determine whether clinical effects of dDBS can be predicted in individual patients based on lead location and volume of tissue activated (VTA) modelling.
*Methods:* We analysed a prospective series of 28 PD patients. Imaging analysis and systematic clinical testing performed 4–6 months postoperatively yielded location, clinical efficacy and corresponding therapeutic windows for 272 directional contacts. We calculated the corresponding VTAs to build a probabilistic stimulation map using voxel-wise statistical analysis.
*Results:* We found a positive and statistically significant correlation between the overlap ratio of a patient's individual stimulation volume and the probabilistic map's sweet spot –defined as the 10% voxels with the highest clinical efficacy values (average Spearman's rho = 0.43, average $p \leq 0.036$). Patients who had a larger therapeutic window with directional compared to omnidirectional stimulation had a larger distance between the electrode and the sweet spot centroid (average distances 2.3 vs. 1.5 mm, $p = 0.0019$).
*Conclusion:* Our analysis provides new insights into how the definition of a probabilistic sweet spot based on directional stimulation data and individual VTA modelling can be applied to predict clinically effective directional stimulation and help guide clinicians with the intricate postoperative DBS programming.



## Introduction

Subthalamic nucleus (STN) deep brain stimulation (DBS) is an effective treatment option for patients with advanced Parkinson's disease (PD) and other movement disorders to alleviate motor symptoms such as slowness of movement, rigidity or tremor [1,2]. Evidence suggests that accurate and precise lead placement in the dorsolateral motor part of the STN is of paramount importance for successful treatment [3–5]. Suboptimal lead placement increases the likelihood of current spread into adjacent structures and hence, stimulation-induced side effects [6]. In addition, finite-element models of electric field distribution have significantly contributed to a better understanding of the volume of tissue activated (VTA) by the stimulating electrodeand how these models could be used to guide and improve stimulation effects [7,8].

Directional DBS (D-DBS) has recently been introduced to overcome some limitations of classical omnidirectional DBS [9]. D-DBS leads have segmented contacts and therefore enable a spatially more confined stimulation via current steering to specific regions of

*Abbreviations:* DBS, deep brain stimulation; PD, Parkinson's disease; MNI, Montreal Neurological Institute; STN, subthalamic nucleus; UPDRS, Unified Parkinson's disease rating scale; VTA, volume of tissue activated.

* Corresponding author.
*E-mail address:* neuro.nowacki@gmail.com (A. Nowacki).

[1] The first two authors contributed equally to this work.

https://doi.org/10.1016/j.brs.2019.05.001
1935-861X/

interest. In contrast to omnidirectional DBS leads, where the stimulation field could be moved primarily along the vertical axis (Z axis), D-DBS provides a unique opportunity to make further anatomico-clinical explorations in the horizontal plane (along the X and Y axes). Stimulation-induced side effects should therefore be reduced and therapeutic window widened when applying D-DBS. The proof of concept that directional stimulation increases the therapeutic window has been shown intraoperatively [10,11]. Subsequent clinical trials with chronically implanted patients have confirmed these results [12,13].

However, the underlying neural mechanisms of the beneficial effects of D-DBS still need to be elucidated. Furthermore, from a clinical perspective it remains unclear under which circumstances individual patients may benefit from directional stimulation over classical omnidirectional stimulation. Furthermore, with the increased number of electrodes, programming becomes more complex and time-consuming when using a "trial-and-error" empirical approach, i.e., a systematic clinical mapping of all electrodes [14]. Thus, a better understanding of the relationship between directional stimulation of neural structures and the clinical responses is needed to help guide programming of DBS devices and fully exploit its therapeutic potential. Therefore, the objective of the current work was to:

1. Determine a probabilistic, clinically effective stimulation site within the STN based on directional stimulation,
2. Determine whether clinical effects of directional stimulation can be predicted in individual patients based on DBS lead location and VTA modelling,
3. Identify factors that indicate whether a subject may benefit from directional stimulation over omnidirectional stimulation.

## Materials and methods

### *Patients*

This monocentric study included 28 consecutive PD patients (19 male, 9 female; mean age 63 ± 9 years, range 48–76) undergoing bilateral DBS of the STN between November 2015 and April 2017. Awake surgery using a Leksell G frame (Elekta instruments, Stockholm, Sweden) with intraoperative use of microelectrode recording and clinical testing was performed in each patient. The D-DBS lead model Boston Vercise Cartesia (Boston Scientific, Marlborough, MA, USA) was implanted. The operative procedure is described in detail elsewhere [15]. Patients' consent was obtained and the local ethics committee approved the study.

### *Clinical contact testing and parameters*

Systematic clinical assessment of monopolar stimulation of each contact was performed 4–6 months (mean 24 ± 6 weeks) after DBS surgery under supervision of a movement disorder neurologist, who was blinded to imaging data and therefore exact lead position and orientation (Fig. 1). Levodopa was stopped at least 12 h, dopamine agonists up to 48 h before clinical testing. Clinical testing consisted of assessment of upper limb tremor and rigidity by passive flexion/extension movements of the elbow and hand wrist. Symptom severity was rated clinically testing according to the Movement Disorders Society Unified Parkinson's Disease Rating Scale (MDS-UPDRS) [16]. Stimulation frequency and pulse width were set to 130 Hz and 60 μs by default. Stimulation amplitude was started at 1 mA and increased stepwise in 0.5 mA increments. At each increment of stimulation amplitude, the patient was tested for occurrence of dysarthria, twitching movements of upper and lower extremities and facial muscles, gaze and diplopia, and paraesthesias. Assessment was performed in two separate sessions on two following days with the first session testing omnidirectional stimulation and a second session testing directional stimulation (i.e., monopolar stimulation of directional electrodes) during a short hospitalisation. A testing session usually took one to two hours. The effect threshold was determined as the stimulation current necessary to completely relieve rigidity or to obtain the best achievable improvement in this clinical sign. The side effect threshold was defined as the stimulation amplitude that provoked either a) significantly impairing dysarthria, b) muscle spasms or twitching of either facial muscles or in the extremities, c) sustained paraesthesia, d) diplopia or e) significant feeling of unease. Therapeutic window was defined as the difference between side effect and effect thresholds. Clinical efficacy was defined according to Eq. (1), where ET denotes effect threshold:

$$clinical\ efficacy = \frac{rigidity\ at\ baseline - rigidity\ at\ ET}{rigidity\ at\ baseline \times Current\ at\ ET} \quad (1)$$

We defined two groups of patients according to clinical testing: patients, who showed a wider therapeutic window with omnidirectional stimulation mode compared to directional stimulation were labelled *group A*, whereas patients who showed a wider therapeutic window with directional stimulation compared to omnidirectional stimulation were labelled *group B*.

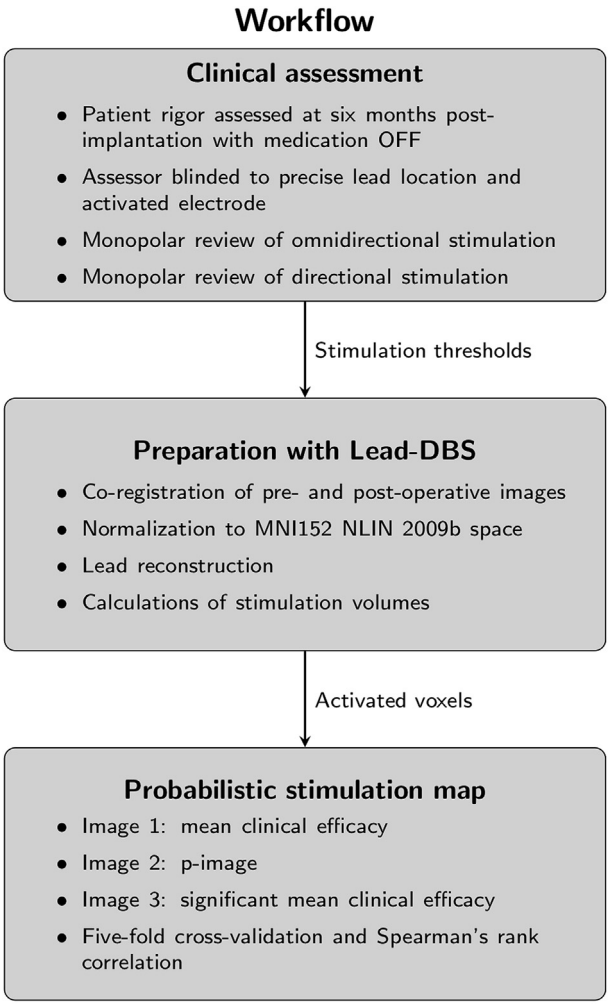


**Fig. 1.** Overview of the workflow.

*Postoperative lead localization and estimation of volume of tissue activated*

An early postoperative high-resolution CT scan performed on the day following surgery was used for DBS lead reconstruction using Lead-DBS toolbox (version 2.1.6) in Matlab 2016b (The Mathworks, Natick, MA, USA) as described recently by our and other groups [17–19]. Leads were semi-automatically localized with the PaCER algorithm [20]. The orientation of the lead was determined with skull X-rays in two planes (anterior-posterior and lateral) performed three to five days following surgery.

The volume of tissue activated was estimated with Lead-DBS based on previous models [21,22]. The assignment to gray and white matter was done based on the DISTAL atlas, as this atlas proved to be of acceptable accuracy compared to patients' individual MRI scans [17,23]. Conductivity values for white matter were set to 0.14 S/mm and for gray matter to 0.33 S/mm [21]. Thresholding of the potential gradient at 0.2 V/mm then determined activated tissue.

*Generation of probabilistic stimulation map*

Methods to create a probabilistic stimulation map have been presented before [24–27]. The map generated here was adapted from work by Eisenstein and coworkers [27]. Briefly, for each patient and stimulation setting we estimated the VTA in MNI template space. Each voxel covered by the VTA was assigned the corresponding clinical efficacy score for that patient and stimulation setting. Voxels not activated by the VTA were assigned a score of 0. Mean clinical efficacy scores were then calculated for each voxel to create a *mean clinical efficacy image*. A voxel-wise Wilcoxon signed rank test (one-tailed, significance level detailed below) was performed to test for statistical significance against zero. P-values for each voxel were displayed in the *p-image*. Finally, a *significant mean clinical efficacy image* was created displaying the mean clinical efficacy per voxel, but taking into account only voxels statistically significant from zero. Voxels with accepted null hypothesis were discarded and their mean clinical efficacy value was set to zero. Voxels with rejected null hypothesis, thus indicating significant clinical effect, were preserved for the probabilistic stimulation map.

Side effect thresholds were used to identify a safe zone of stimulation with minimal probability of evoking side effects. This information was then integrated into the map described above. Using the thresholds from clinical mapping, we first estimated VTAs at side effect threshold minus 0.5 mA, i.e., the highest current amplitude tested that did not elicit side effects. Finally this safe stimulation zone was fused into the map above. Voxels that were outside the safe zone were now marked with a mean clinical efficacy score of −1 representing a penalty when activated.

*Sweet spot and correlation to clinical efficacy*

To determine the predictive value of the map, we defined *overlap ratio* as the volume overlap of an individual VTA and the probabilistic sweet spot divided by the individual VTA volume. The overlap ratio was calculated as in Eq. (2).

$$\textit{overlap ratio} = \frac{\textit{Volume overlap between VTA and hot spot}}{\textit{Volume of VTA}} \quad (2)$$

This sweet spot was defined from the map by identifying voxels with a mean clinical efficacy value at the 90th percentile or above (Fig. 4). In other words this represented the top ten percent of voxels. We also evaluated sweet spots defined at the 80$^{th}$ or 95th percentile, but opted for the 90$^{th}$ percentile as cut-off due to the sweet spot volume (48, 12 and 24 mm$^3$, respectively). Thus we considered the 90$^{th}$ percentile to be most meaningful and tangible given the volume of the STN of about 120 mm$^3$ with the DISTAL atlas in MNI template space.

Overlap ratio was correlated to individual clinical efficacy values. To better test this correlation and reduce variability of correlation results, we used a five-fold cross-validation [28]. We randomly divided our data into five blocks of approximately the same size (e.g., blocks were labelled A through E). A probabilistic stimulation map was then generated from four of these blocks corresponding to approximately 80% of the data (e.g., blocks A through D). This is usually referred to as training in machine learning. Then correlations were computed with the remaining block corresponding to approximately 20% of the data (e.g., block E). This is usually referred to as testing in machine learning. Importantly, this block was not used during map generation and therefore the map was not fitted to or biased towards that data. This training and testing was performed five times in total, so that each block was used exactly once for testing. For example in a second round, the map was generated with data from blocks A, B, C and E, and testing was performed with block D. Specifically for this study, we excluded patients who were symptom free at the beginning of the clinical testing (baseline rigidity 0). This yielded VTA estimations for 272 directional contacts (144 for left and 128 for right hemisphere). Spearman's rank correlation was performed between the clinical efficacy value and the two variables defined above. This was repeated for each fold of cross-validation. All computations were performed in Matlab 2016b.

*Statistical analyses*

For the generation of the probabilistic stimulation map, the mean clinical efficacy image comprised 140x140x140 voxels and more than two million voxel-wise Wilcoxon signed rank tests were calculated. To reduce type I errors due to multiple testing, we adopted a false discovery rate as described in detail elsewhere [29,30]. The Spearman's rank correlation coefficients from the five-fold cross-validation were averaged through Fisher's z transformation. The corresponding p-values were averaged conservatively with an arithmetic mean multiplied by 2.

## Results

Twenty-eight consecutive PD patients undergoing bilateral STN DBS were included in the final analysis. Ten hemispheres and four additional directional contacts had to be excluded from the map generation due to missing symptoms at baseline or lack of patient compliance during testing due to exhaustion. Furthermore, for the Group A versus Group B analysis, six hemispheres were excluded that did not yield therapeutic windows during clinical testing. In total, VTA estimations for 272 directional contact stimulation and for 50 omnidirectional configurations were analysed leading to a total of 322 different stimulation settings. The mean preoperative "medication off" MDS-UPDRS score was 38.6 ± 14.6. The mean postoperative "medication off-stimulation on" MDS-UPDRS score was 22.6 ± 9.3 ($p < 0.0001$).

In 24 of 56 (43%) analysed hemispheres directional stimulation provided a larger therapeutic window compared to omnidirectional stimulation. *Group A* patients who had a similar or smaller therapeutic window with directional stimulation (1.6 ± 1.0 mA) compared to omnidirectional (2.1 ± 0.9 mA) stimulation and thus did *not benefit* from directional stimulation during our acute clinical testing. *Group B* patients had a larger therapeutic window with directional stimulation (2.1 ± 1.58 mA) compared to omnidirectional (1.38 ± 1.15 mA) stimulation and thus *did benefit* from

directional stimulation. We could not consistently find a lower effect threshold or higher side-effect threshold that accounted for the overall increased therapeutic window in *Group B* patients.

### *Contact location*

The anatomical location of all contacts was analysed (Fig. 2). Most contacts were accumulated in the middle third on the anterior-posterior axis of the nucleus reflecting the targeting approach of the surgeon. Directional contacts that attained full clinical effect (complete rigidity reduction) had different locations along the dorsoventral axis than contacts that attained partial effect only, the latter ones being located in the ventral part more frequently (Fig. 2).

### *Probabilistic stimulation map*

The probabilistic stimulation map was computed using the VTAs of directional contacts (Fig. 3). The mean clinical efficacy image had voxels with non-zero mean clinical efficacy both in- and outside the STN (Fig. 3A and B). Following multiple comparison in the p-image (Fig. 3C and D), significantly effective voxels were kept for the significant mean clinical efficacy image (Fig. 3 E,F). This image was combined with a safe zone of stimulation. Notably, significantly effective voxels with high mean clinical efficacy values were located in the dorsolateral part of the STN. A 'neutral zone' followed with voxels that had no significant clinical effect, but were within the safe zone of stimulation (red transparent zone in Fig. 3E and F).

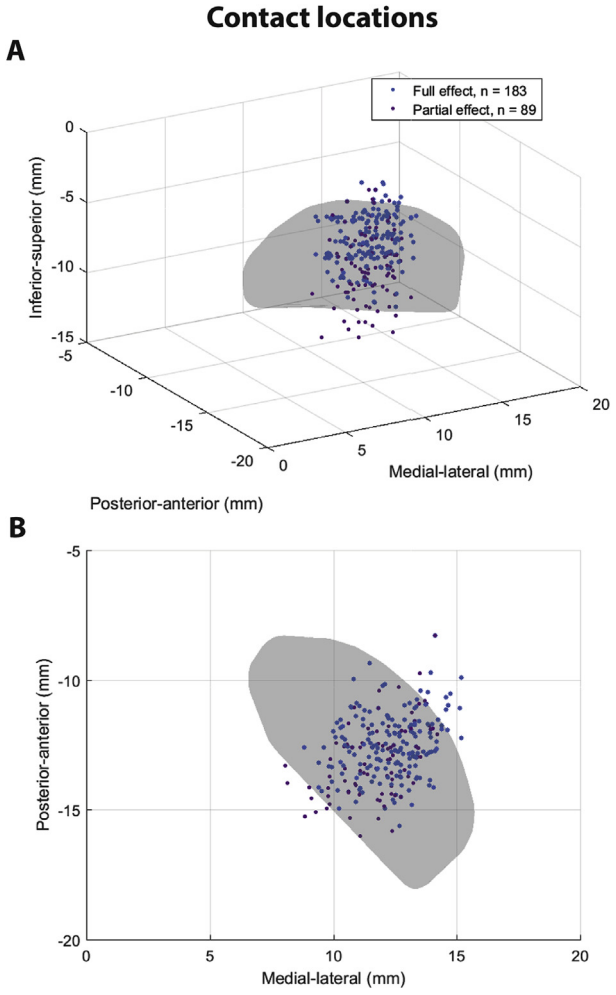


**Fig. 2.** Location of all directional contacts projected in MNI template space and right subthalamic nucleus in gray. Contacts whose activation achieved full effect (100% rigidity reduction) are marked blue and those whose activation achieved partial effect are marked red. (For interpretation of the references to colour in this figure legend, the reader is referred to the Web version of this article.)

### *Sweet spot and correlation with clinical efficacy*

We found significant moderate correlation between overlap ratio and clinical efficacy (Fig. 4). This sweet spot defined by voxels at the 90$^{th}$ percentile and above had a volume of 24.1 mm$^3$ and may be described as an ellipsoid with lengths of about 5 mm, 3.3 mm and 4 mm along the principal axes. Greater overlap ratio was associated with greater clinical efficacy (average Spearman's rho = 0.43, average $p \leq 0.036$). Notably, four folds of the cross-validation returned a p-value below the significance level of 0.05, only the third fold had a p-value of 0.07. All correlation coefficients and p-values are listed in Table 1.

### *Benefit from directional stimulation*

*Group A* and *group B* patients showed differences in contact position and overlap ratio. Group A patients were on average 0.8 mm closer to the centroid of the probabilistic sweet spot than group B (average distances 1.5 vs. 2.3 mm, respectively, *t*-test, $p = 0.0019$, Fig. 5A–C).

The overlap ratio in group A was highest for omnidirectional stimulation compared to directional stimulation. The difference with best directional stimulation (directional contact with largest therapeutic window) was not significant (one-way ANOVA, $p = 0.24$), while the difference with worst directional stimulation was significant ($p < 0.001$). Conversely, the overlap ratio in group B was highest for best directional stimulation compared to omnidirectional stimulation ($p = 0.99$) and worst directional stimulation ($p = 0.002$, Fig. 5D).

## Discussion

We developed a probabilistic stimulation map for clinically effective D-DBS in the STN area of chronically implanted PD patients. Our findings are based on clinical testing of different stimulation settings comparing directional and omnidirectional stimulation. Using VTA estimations from 272 directional contacts, we were able to generate a highly detailed probabilistic stimulation map of the STN. We showed that the probabilistic stimulation volume for directional stimulation associated with the highest clinical efficacy projected onto the dorsolateral STN. The *overlap ratio* between an individual VTA and the stimulation sweet spot was positively correlated with clinical efficacy. Notably, this parameter and the electrode distance to the sweet spot centroid were helpful indicators of whether a patient would benefit from directional stimulation over omnidirectional stimulation.

### *Generation of probabilistic stimulation map*

The generation of our probabilistic stimulation map was based on previous work by Eisenstein and coworkers, [27]. In contrast to their work, our map was based on directional stimulation, which allowed for refined spatial mapping, especially in both horizontal axes (X and Y axes). To further improve spatial resolution, we used a finite-element model to estimate volume of tissue activated, whereas their analysis assumed a spherical activation volume weighted with a Gaussian function.

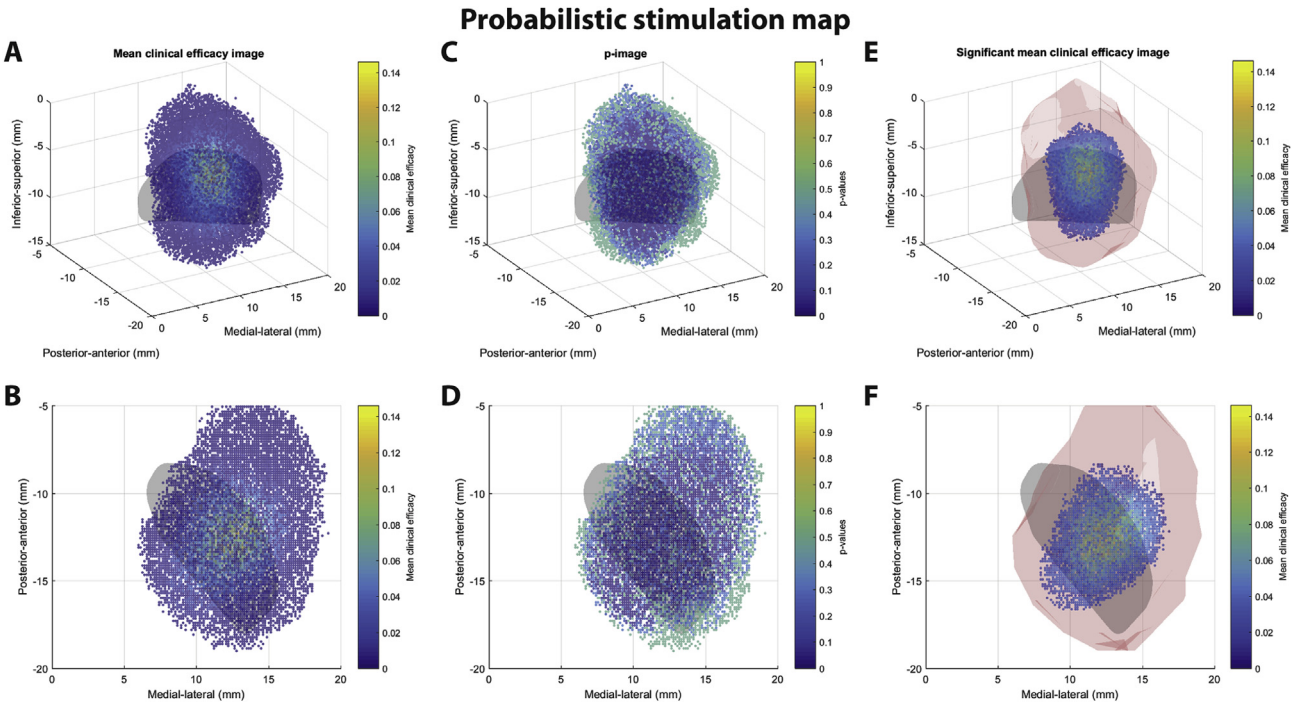


**Fig. 3.** Generation of the probabilistic stimulation map. Top row shows a pseudo three-dimensional view of the subthalamic nucleus in gray and voxels of the three images, while bottom row showing an axial view of the corresponding image above.Images represent the first fold of the cross-validation. (A, B) Mean clinical efficacy image; (C, D) p-image. Preserving voxels with significant values resulted in the significant mean clinical efficacy image (E, F) that also shows the 'neutral zone' of stimulation as transparent red volume. (For interpretation of the references to colour in this figure legend, the reader is referred to the Web version of this article.)

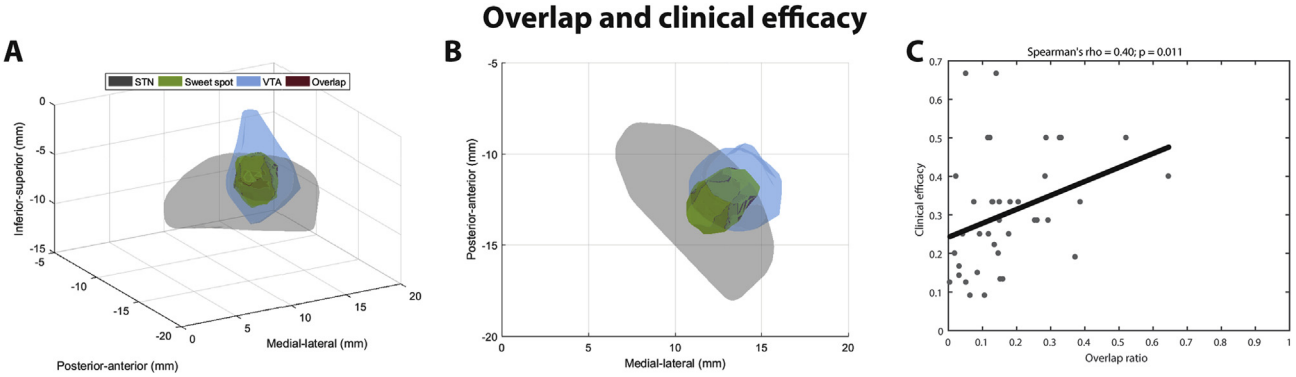


**Fig. 4.** In the testing part of cross-validation, overlap ratio was correlated with clinical efficacy. (A, B) Views of one VTA (blue) overlapping with the probabilistic stimulation sweet spot (green). The overlap is plotted in red and the overlap ratio in this case was approx. 0.33. (C) Correlation of overlap ratio with clinical efficacy from the first fold of cross-validation. Statistics for all folds listed in Table 1. (For interpretation of the references to colour in this figure legend, the reader is referred to the Web version of this article.)

**Table 1**
Correlation coefficients from cross-validation. Overlap ratio was calculated for a sweet spot defined by 90$^{th}$ percentile.* Mean p-values were conservatively estimated as explained in Methods.

| Fold | Overlap ratio | |
|---|---|---|
| | Spearman's rho | p-value |
| 1 | 0.4 | 0.011 |
| 2 | 0.61 | 1.1e-5 |
| 3 | 0.27 | 0.071 |
| 4 | 0.46 | 0.001 |
| 5 | 0.39 | 0.007 |
| Mean | 0.43 | ≤0.036* |

Probabilistic stimulation maps were recently generated for DBS in essential tremor [26]. Based on omnidirectional stimulation, the group created two sets of maps: one set to identify effective stimulation targets for tremor suppression; and a second set to identify regions with high occurrence of stimulation-induced side effects such as paraesthesia or dizziness. Here, we did not distinguish between different types of side effects, but instead decided to define a safe zone of stimulation and combine these two sets of maps together. This yielded a map with a layer of voxels that had significant clinical efficacy, a second layer of voxels that had non-significant clinical efficacy (neutral zone) and a third layer of voxels that had a high likelihood of inducing side-effects (Fig. 3). As expected, voxels likely to induce side-effects projected onto areas lateral and caudal to the STN, thus reflecting the anatomical

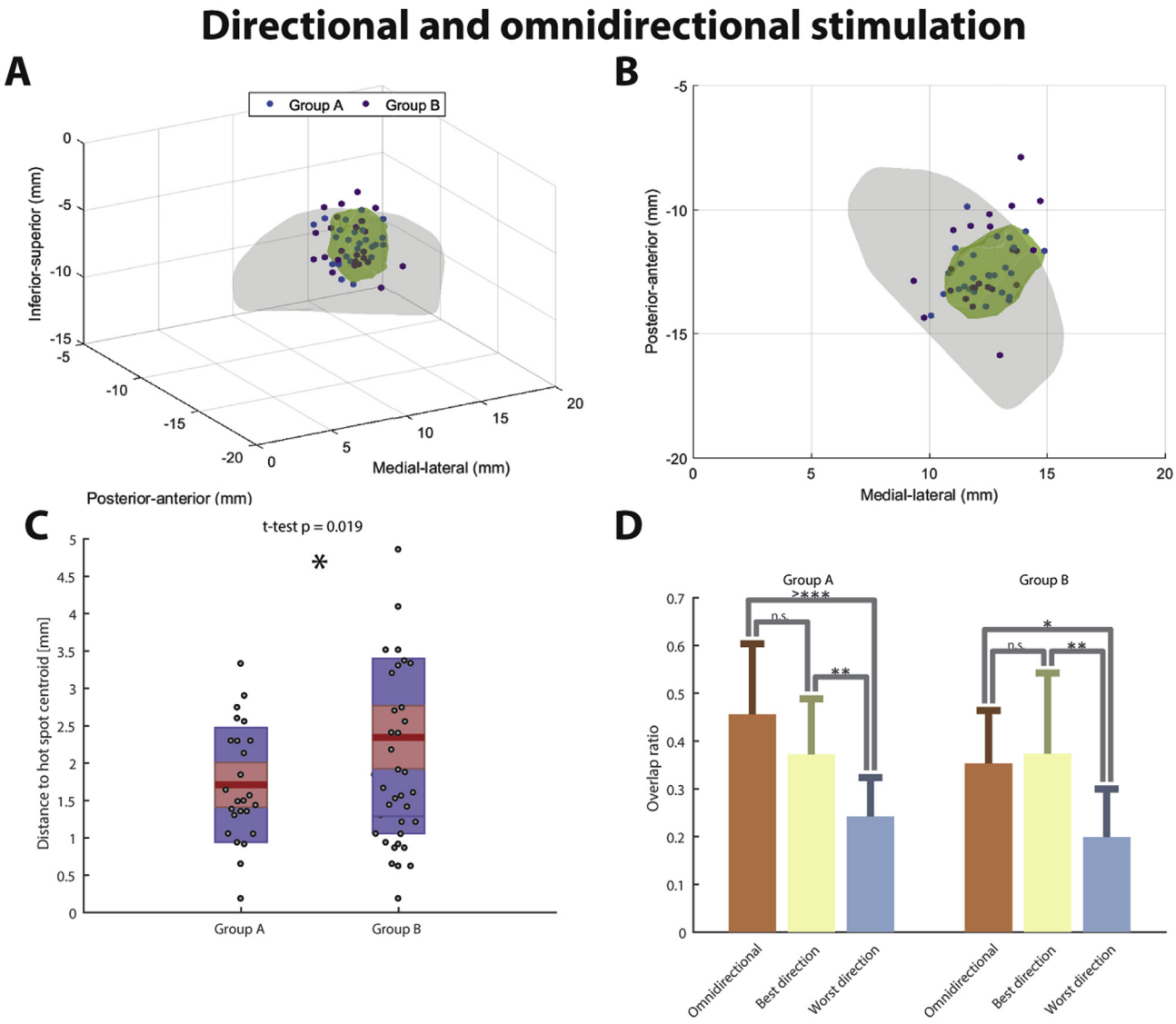


**Fig. 5.** Comparison of directional and omnidirectional stimulation. Patients in group A did not benefit from directional stimulation, whereas patients in group B did. (A, B) Location of contacts with the largest therapeutic window per patient with respect to the probabilistic stimulation sweet spot (green). Group A (blue) was located significantly closer to the sweet spot centroid than group B (purple). (C) Mean distance of group A to the centroid was 1.5 mm versus 2.3 mm for group B. Dots show individual contacts, boxes represent mean with standard error of the mean. (D) Overlap ratio for omnidirectional, best and worst directional stimulation for groups A and B. (For interpretation of the references to colour in this figure legend, the reader is referred to the Web version of this article.)

locations of the internal capsule and substantia nigra. Future versions of the map may fine-tune this value to reflect different types and severity of side effects.

### *Correlation with clinical efficacy*

The clinical usefulness of a probabilistic map that exclusively reflects *population*-based likelihoods may be questioned. Each individual patient responds differently to DBS. We tested whether the probabilistic stimulation map can provide a predictive value for *individual* patients. We found that the overlap ratio with the stimulation sweet spot was positively correlated with individual clinical efficacy. This suggests a useful marker to predict effective stimulation settings in an individual patient.

Our probabilistic stimulation sweet spot represented a volume that was associated with most effective rigidity reduction. It projected onto the dorsolateral STN and confirmed findings of previous studies [4,5]. More recently, several studies of PD patients undergoing STN DBS used resting state fMRI and diffusion-weighted imaging to perform probabilistic functional and structural connectivity analysis. For instance, Acolla et al. found that different anatomically and electrophysiologically defined subregions of the STN have a distinct connectivity profile to certain cortical regions. Based on this, Horn and coworkers found that connectivity between the DBS electrode and a distributed network of brain regions including the supplementary motor cortex, prefrontal cortex, and anterior cingulate cortex correlates with clinical outcome [31]. Akram and coworkers found that clinical response of rigidity, tremor and bradykinesia was associated with different cortical connectivity profiles [32]. In the present study we did not conduct probabilistic structural or functional connectivity analysis and therefore plan to evaluate whether connectivity may provide any additional predictive value in future studies.

*Predictors of effective directional stimulation*

Directional stimulation provided a slightly increased therapeutic window with a lower effect threshold compared to omnidirectional stimulation. Across our cohort, 43% of patients benefitted from directional stimulation during clinical mapping and showed an increased therapeutic window compared to omnidirectional stimulation. We found that directional contacts of group B patients were anatomically more distant from the sweet spot centroid than contacts of group A patients. This indicated that directional stimulation can alleviate situations where the lead is possibly placed sub-optimally, in group B patients with a mean distance of 2.3 mm from the centroid. This is in accordance with Anderson et al. who demonstrated in-silico that directional stimulation can achieve better target activation than omnidirectional stimulation, in particular when the lead was placed 2 mm off-target [33]. One possible explanation is the distinct capability of directional leads to steer stimulation intentionally towards regions of interest and away from regions of avoidance as hypothesized by Steigerwald and Anderson [12,33].

Second, we were particularly interested whether individual VTA models can help understand why and under what circumstances some patients profit from directional stimulation. The overlap ratio was a useful indicator. Group A patients had slightly larger overlap ratio with omnidirectional stimulation than best directional stimulation. Conversely, group B patients had slightly higher values with best directional stimulation than omnidirectional stimulation. This finding was in line with the hypothesis that directional stimulation can compensate for sub-optimally placed leads. It also underlined the capability of directional stimulation to better target regions of interest to enhance overlap ratio in group B patients.

*Limitations*

Our study has several limitations. First, a problem inherent to the conception of a probabilistic stimulation map, which is based on clinical data, is that the probabilistic distribution and sweet spot solely reflect the distribution of implanted electrodes. These are usually distributed around the intended target selected by the surgeon. This was also evident in our series of patients in which most electrodes were distributed in the middle third of the anterior-posterior axis of the nucleus. As a consequence the probabilistic map may favour the targeted area over the undersampled surrounding area. We minimized this problem by 1) taking into account data from all available contacts and not only the most effective ones, 2) by taking into account sub-optimal stimulation settings such as side-effect thresholds, 3) reducing type-1-error of multiple testing by applying a false discovery rate. The method presented here for the probabilistic stimulation map may work for Parkinson's disease and the subthalamic nucleus. However, it may have to be adapted for other indications or targets, where VTAs are sparser."

Second, clinical efficacy was defined as the degree of rigidity reduction per stimulation amplitude to obtain the maximum possible rigidity reduction with a given contact. Thus, clinical efficacy measures only one aspect of PD at a very limited time point and did not take into account other beneficial stimulation effects. However, in a short mapping rigidity is the only clinical sign that can be assessed reliably and rapidly. On the other hand, bradykinesia can only be assessed over a longer time-frame and tremor is fluctuating and strongly influenced by emotion and therefore less reliable. Thus, assessing rigidity reflects the current clinical standard to assess the most effective clinical contact for long-term stimulation [34]. To what extent a probabilistic map based on long-term outcome data incorporating the entire MDS-UPDRS score may differ from the current map based on six month data will be assessed in a follow-up study.

Third, the current analysis used a widely accepted simplified VTA model [21,35]. More accurate models exist that could improve our results but these models come at the expense of a significantly increased computational demand [24,36].

Furthermore, the directionality of the lead was determined based on the postoperative skull x-ray in two planes. We were not able to exclude a further rotation of the lead over a longer period of time. This particular point should be investigated in a longer time-frame." This inevitably leads to imprecise estimations of the lead orientation in the range of 15–30° and might lead to distortions of the VTA and the probabilistic stimulation volume. Recently, an algorithm based on postoperative rotational 3D fluoroscopy allowed for determining the orientation of the leads more precisely [37].

The presented results are from a limited number of patients from only one DBS centre and thus not generalizable to a broader population.

## Conclusions

We were able to generate a probabilistic stimulation map of the STN based on clinical mapping results of directional electrodes, which were correlated to computer models of directional stimulation. We identified a confined stimulation area (sweet spot) located in the dorsolateral part of the STN. An optimised overlap between an individual VTA and the sweet spot was significantly correlated with clinical efficacy for rigidity. Directional stimulation of the probabilistic sweet spot may therefore predict clinically effective DBS and indicate whether a subject may benefit from directional stimulation over omnidirectional stimulation. In this respect, our map may be used in clinical practice to optimise directional lead programming using a probabilistic instead of a "trial-and-error" empirical programming approach. This approach may decrease the complexity and the time needed for programming of DBS for Parkinson's disease patients. This proof of concept study warrants additional data from multiple centres as well as a randomized prospective multicentre comparison of both programming approaches to confirm and refine our results.

## Declarations of interest

None.

## Appendix A. Supplementary data

Supplementary data to this article can be found online at https://doi.org/10.1016/j.brs.2019.05.001.

## References

[1] Deuschl G, Schade-Brittinger C, Krack P, Volkmann J, Schafer H, Botzel K, et al. A randomized trial of deep-brain stimulation for Parkinson's disease. N Engl J Med 2006;355:896–908. https://10.1056/NEJMoa060281.

[2] Schuepbach WM, Rau J, Knudsen K, Volkmann J, Krack P, Timmermann L, et al. Neurostimulation for Parkinson's disease with early motor complications. N Engl J Med 2013;368:610–22. https://10.1056/NEJMoa1205158.

[3] Welter ML, Schupbach M, Czernecki V, Karachi C, Fernandez-Vidal S, Golmard JL, et al. Optimal target localization for subthalamic stimulation in patients with Parkinson disease. Neurology 2014;82:1352–61. https://10.1212/WNL.0000000000000315.

[4] Wodarg F, Herzog J, Reese R, Falk D, Pinsker MO, Steigerwald F, et al. Stimulation site within the mri-defined stn predicts postoperative motor outcome. Mov Disord 2012;27:874–9. https://10.1002/mds.25006.

[5] Bot M, Schuurman PR, Odekerken VJJ, Verhagen R, Contarino FM, De Bie RMA, et al. Deep brain stimulation for Parkinson's disease: defining the optimal location within the subthalamic nucleus. J Neurol Neurosurg Psychiatry 2018;89:493–8. https://10.1136/jnnp-2017-316907.

[6] Fitzpatrick JM, Konrad PE, Nickele C, Cetinkaya E, Kao C. Accuracy of customized miniature stereotactic platforms. Stereotact Funct Neurosurg 2005;83:25–31. https://10.1159/000085023.
[7] Frankemolle AM, Wu J, Noecker AM, Voelcker-Rehage C, Ho JC, Vitek JL, et al. Reversing cognitive-motor impairments in Parkinson's disease patients using a computational modelling approach to deep brain stimulation programming. Brain 2010;133:746–61. https://10.1093/brain/awp315.
[8] Maks CB, Butson CR, Walter BL, Vitek JL, McIntyre CC. Deep brain stimulation activation volumes and their association with neurophysiological mapping and therapeutic outcomes. J Neurol Neurosurg Psychiatry 2009;80:659–66. https://10.1136/jnnp.2007.126219.
[9] Schupbach WMM, Chabardes S, Matthies C, Pollo C, Steigerwald F, Timmermann L, et al. Directional leads for deep brain stimulation: opportunities and challenges. Mov Disord 2017;32:1371–5. https://10.1002/mds.27096.
[10] Pollo C, Kaelin-Lang A, Oertel MF, Stieglitz L, Taub E, Fuhr P, et al. Directional deep brain stimulation: an intraoperative double-blind pilot study. Brain 2014;137:2015–26. https://10.1093/brain/awu102.
[11] Contarino MF, Bour LJ, Verhagen R, Lourens MA, de Bie RM, van den Munckhof P, et al. Directional steering: a novel approach to deep brain stimulation. Neurology 2014;83:1163–9. https://10.1212/WNL.0000000000000823.
[12] Steigerwald F, Muller L, Johannes S, Matthies C, Volkmann J. Directional deep brain stimulation of the subthalamic nucleus: a pilot study using a novel neurostimulation device. Mov Disord 2016;31:1240–3. https://10.1002/mds.26669.
[13] Dembek TA, Reker P, Visser-Vandewalle V, Wirths J, Treuer H, Klehr M, et al. Directional dbs increases side-effect thresholds-a prospective, double-blind trial. Mov Disord 2017;32:1380–8. https://10.1002/mds.27093.
[14] Ten Brinke TR, Odekerken VJJ, Dijk JM, van den Munckhof P, Schuurman PR, de Bie RMA. Directional deep brain stimulation: first experiences in centers across the globe. Brain Stimul 2018;11:949–50. https://10.1016/j.brs.2018.04.008.
[15] Nowacki A, Debove I, Fiechter M, Rossi F, Oertel MF, Wiest R, et al. Targeting accuracy of the subthalamic nucleus in deep brain stimulation surgery: comparison between 3 t t2-weighted magnetic resonance imaging and microelectrode recording results. Oper Neurosurg (Hagerstown) 2017. https://doi.org/10.1093/ons/opx175.
[16] Goetz CG, Tilley BC, Shaftman SR, Stebbins GT, Fahn S, Martinez-Martin P, et al. Movement disorder society-sponsored revision of the unified Parkinson's disease rating scale (mds-updrs): Scale presentation and clinimetric testing results. Mov Disord 2008;23:2129–70. https://10.1002/mds.22340.
[17] Nowacki A, Nguyen TA, Tinkhauser G, Petermann K, Debove I, Wiest R, et al. Accuracy of different three-dimensional subcortical human brain atlases for dbs -lead localisation. Neuroimage Clin 2018;20:868–74. https://10.1016/j.nicl.2018.09.030.
[18] Horn A, Kuhn AA. Lead-dbs: a toolbox for deep brain stimulation electrode localizations and visualizations. Neuroimage 2015;107:127–35. https://10.1016/j.neuroimage.2014.12.002.
[19] Avants BB, Epstein CL, Grossman M, Gee JC. Symmetric diffeomorphic image registration with cross-correlation: evaluating automated labeling of elderly and neurodegenerative brain. Med Image Anal 2008;12:26–41. https://10.1016/j.media.2007.06.004.
[20] Husch A, P MV, Gemmar P, Goncalves J, Hertel F. Pacer - a fully automated method for electrode trajectory and contact reconstruction in deep brain stimulation. Neuroimage Clin 2018;17:80–9. https://10.1016/j.nicl.2017.10.004.
[21] Astrom M, Diczfalusy E, Martens H, Wardell K. Relationship between neural activation and electric field distribution during deep brain stimulation. IEEE Trans Biomed Eng 2015;62:664–72. https://10.1109/TBME.2014.2363494.
[22] Ewert S, Plettig P, Li N, Chakravarty MM, Collins DL, Herrington TM, et al. Toward defining deep brain stimulation targets in mni space: a subcortical atlas based on multimodal mri, histology and structural connectivity. Neuroimage 2018;170:271–82. https://10.1016/j.neuroimage.2017.05.015.
[23] Ewert S, Plettig P, Li N, Chakravarty MM, Collins DL, Herrington TM, et al. Toward defining deep brain stimulation targets in mni space: a subcortical atlas based on multimodal mri, histology and structural connectivity. Neuroimage 2017. https://doi.org/10.1016/j.neuroimage.2017.05.015.
[24] Butson CR, Cooper SE, Henderson JM, Wolgamuth B, McIntyre CC. Probabilistic analysis of activation volumes generated during deep brain stimulation. Neuroimage 2011;54:2096–104. https://10.1016/j.neuroimage.2010.10.059.
[25] Cheung T, Noecker AM, Alterman RL, McIntyre CC, Tagliati M. Defining a therapeutic target for pallidal deep brain stimulation for dystonia. Ann Neurol 2014;76:22–30. https://10.1002/ana.24187.
[26] Dembek TA, Barbe MT, Astrom M, Hoevels M, Visser-Vandewalle V, Fink GR, et al. Probabilistic mapping of deep brain stimulation effects in essential tremor. Neuroimage Clin 2017;13:164–73. https://10.1016/j.nicl.2016.11.019.
[27] Eisenstein SA, Koller JM, Black KD, Campbell MC, Lugar HM, Ushe M, et al. Functional anatomy of subthalamic nucleus stimulation in Parkinson disease. Ann Neurol 2014;76:279–95. https://10.1002/ana.24204.
[28] Krstajic D, Buturovic LJ, Leahy DE, Thomas S. Cross-validation pitfalls when selecting and assessing regression and classification models. J Cheminf 2014;6:10. https://10.1186/1758-2946-6-10.
[29] Genovese CR, Lazar NA, Nichols T. Thresholding of statistical maps in functional neuroimaging using the false discovery rate. Neuroimage 2002;15:870–8. https://10.1006/nimg.2001.1037.
[30] Rowe DB, Logan BR. A complex way to compute fmri activation. Neuroimage 2004;23:1078–92. https://10.1016/j.neuroimage.2004.06.042.
[31] Horn A, Reich M, Vorwerk J, Li N, Wenzel G, Fang Q, et al. Connectivity predicts deep brain stimulation outcome in Parkinson disease. Ann Neurol 2017;82:67–78. https://10.1002/ana.24974.
[32] Akram H, Sotiropoulos SN, Jbabdi S, Georgiev D, Mahlknecht P, Hyam J, et al. Subthalamic deep brain stimulation sweet spots and hyperdirect cortical connectivity in Parkinson's disease. Neuroimage 2017;158:332–45. https://10.1016/j.neuroimage.2017.07.012.
[33] Anderson DN, Osting B, Vorwerk J, Dorval AD, Butson CR. Optimized programming algorithm for cylindrical and directional deep brain stimulation electrodes. J Neural Eng 2018;15:026005. https://10.1088/1741-2552/aaa14b.
[34] Picillo M, Lozano AM, Kou N, Munhoz RP, Fasano A. Programming deep brain stimulation for tremor and dystonia: the toronto western hospital algorithms. Brain Stimul 2016;9:438–52. https://10.1016/j.brs.2016.02.003.
[35] Hemm S, Coste J, Gabrillargues J, Ouchchane L, Sarry L, Caire F, et al. Contact position analysis of deep brain stimulation electrodes on post-operative ct images. Acta Neurochir 2009;151:823–9. discussion 829, https://10.1007/s00701-009-0393-3.
[36] Howell B, McIntyre CC. Analyzing the tradeoff between electrical complexity and accuracy in patient-specific computational models of deep brain stimulation. J Neural Eng 2016;13:036023. https://10.1088/1741-2560/13/3/036023.
[37] Reinacher PC, Kruger MT, Coenen VA, Shah M, Roelz R, Jenkner C, et al. Determining the orientation of directional deep brain stimulation electrodes using 3d rotational fluoroscopy. AJNR Am J Neuroradiol 2017;38:1111–6. https://10.3174/ajnr.A5153.